Available online at www.sciencedirect.com
SCIENCE DIRECT®
Journal of the European Ceramic Society 25 (2005) 37–47
www.elsevier.com/locate/jeurceramsoc

$M_2(Si,Al)_4(N,C)_7$ (M = La,Y,Ca) carbonitrides I. Synthesis and structural characterisation by XRD and NMR

Kath Liddell [a,*], Derek P. Thompson [a], Thomas Bräuniger [b], Robin K. Harris [b]

[a] *Advanced Materials Division, Department of Chemical Engineering and Advanced Materials, University of Newcastle, Newcastle upon Tyne NE1 7RU, UK*
[b] *Department of Chemistry, University of Durham, South Road, Durham, DH1 3LE, UK*

Received 4 June 2003; received in revised form 6 March 2004; accepted 13 March 2004
Available online 18 May 2004

Abstract

A series of new nitrides and carbonitrides has been identified with crystal structures similar to those of the hexagonal quaternary nitrides of the type (Ba,Sr,Eu)$YbSi_4N_7$. The large divalent cations in these structures can be replaced by trivalent cations such as Ln and/or Y, if valency balance is preserved by the simultaneous substitution of carbon for nitrogen in the unique [4]-coordinated anion site. This has been demonstrated by carbon-13 magic-angle spinning NMR spectra which for the yttrium member of this series shows a peak at 36.7 ppm corresponding to carbon atoms occupying the central non-metal atom site in the characteristic [$C(NSi_3)_4$] structural unit. The resulting compounds have compositions of the types $La_2Si_4N_6C$, $Y_2Si_4N_6C$ or $(La,Y)_2Si_4N_6C$; the crystal structure of a related mixed (Ca,Y) derivative of composition $(Ca,Y)_2Si_4(N,C)_7$ is reported in Part II of this series. When the two large cations are different, the hexagonal symmetry characteristic of the (Ba,Sr,Eu)$YbSi_4N_7$ compounds is maintained; when both cations are the same, lower symmetries are observed. The powder diffraction pattern of $La_2Si_4N_6C$ indexes on an orthorhombic unit cell with $a = 6.0360(7)$, $b = 10.1246(9)$, $c = 10.5664(11)$ Å and the crystal structure has been determined. An alternative way of achieving valency balance without incorporation of carbon is to replace some of the silicon by aluminium; related derivatives of the type $M_2Si_3AlN_7$, where M = La, Y or mixed La,Y have been prepared and their unit cell dimensions are reported.

Keywords: Nitrides; Carbonitrides; XRD; MAS NMR

1. Introduction

Over the last three decades the oxides of yttrium and the rare earths have been used as additives for the densification of silicon nitride and sialon ceramics and phase relationship studies in M_2O_3–SiO_2–Si_3N_4 systems with M = Y,Ln have shown that in addition to Si_2N_2O and the various polymorphic forms of the ternary silicates,[1] there is a range of quaternary phases in these systems such as N-apatite ($M_5Si_3O_{12}N$), N-YAM ($M_4Si_2O_7N_2$) and N-wollastonite ($MSiO_2N$).[2–6] A fourth phase, N-melilite ($M_2Si_3O_3N_4$), is unstable in the La-system and instead the phase $La_3Si_8N_{11}O_4$.[7,8] occurs. The Ce-system contains both $Ce_2Si_3O_3N_4$ and $Ce_3Si_8N_{11}O_4$ phases.[6]

These compounds are those observed in the oxygen-rich half of the M_2O_3–SiO_2–Si_3N_4–MN section of the Jänecke prism. It is more difficult to prepare nitrogen-rich quaternary phases without the use of the binary metal nitrides, which are invariably subject to hydrolysis during use. Nevertheless, yttrium nitride has been used, together with Y_2O_3 and Si_3N_4 at 1800–1900 °C, to investigate the nitrogen-rich region of the Y–Si–O–N system.[9] New phases were observed along the YN–Si_3N_4 join, originally reported as having the compositions "YSi_3N_5" (hexagonal: $a = 9.814$, $c = 10.621$ Å), "$Y_6Si_3N_{10}$" (orthorhombic: $a = 9.854$, $b = 10.288$, $c = 5.978$ Å) and "$Y_2Si_3N_6$" (uncharacterised). The unit cell dimensions of "YSi_3N_5" are similar to those of rare earth silicon oxynitrides of the type $M_6Si_{11}N_{20}O$ and $M_{6.33}Si_{11}N_{21}$ (M = Y,Gd–Lu),[10] and recent work has established[11] that the phase "YSi_3N_5" may contain a small amount of oxygen and have a composition in the range $Y_6Si_{11}N_{20}O$–$Y_3Si_6N_{11}$. Likewise, the phase "$Y_2Si_3N_6$" was found by single-crystal structure determination to have the composition $Y_3Si_5N_9O$.[11] Subsequent preparation of these compounds using the carbo-thermal reduction and ni-

* Corresponding author.
E-mail address: Kath.Liddell@ncl.ac.uk (K. Liddell).

0955-2219/$ – see front matter © 2004 Elsevier Ltd. All rights reserved.
doi:10.1016/j.jeurceramsoc.2004.03.009

tridation process (CRN)[12] has shown that the composition of "$Y_6Si_3N_{10}$" is much less Y-rich than previously supposed and a revised Y:Si ratio of about 1:2 was suggested, inferring a composition close to $Y_3Si_6N_{11}$.

These investigations have been extended into rare-earth silicon oxynitride systems. Phase relationships in the Si_3N_4–Y_2O_3–La_2O_3 system[13] at 1750 °C included an additional phase, C, reported to have a composition near $0.4Y_2O_3{\cdot}0.6La_2O_3{\cdot}3Si_3N_4$. Unindexed X-ray diffraction (XRD) data were reported for this phase; however, the pattern could be indexed on a hexagonal unit cell with $a = 6.03$, $c = 9.92$ Å, almost identical to that of the "$Y_6Si_3N_{10}$" phase discussed above. A similar phase has been observed by the same authors[14] on substituting Yb for Y. In this case the a axis of the hexagonal unit cell was doubled ($a = 11.994$, $c = 9.842$ Å), even though the quoted powder pattern could be indexed on a unit cell with half this a value.

Research in similar mixed cation systems was also reported[15] for starting mixes containing SiC particles. A Si_3N_4–SiC starting mix was sintered with additions of La_2O_3–Y_2O_3–Al_2O_3 at 1750 °C and produced, along with other minor products, a phase analogous to the C-phase above, with unit cell dimensions of $a = 6.012$, $c = 9.896$ Å. During the course of this work, the authors also explored compositions close to that of phase before C and found a maximum amount of this phase in the starting composition $0.4Y_2O_3{\cdot}0.6La_2O_3{\cdot}3Si_3N_4$, sintered at 1500–1650 °C for 4 h. The composition $LaN{\cdot}YN{\cdot}Si_3N_4$, prepared solely from nitrides (the LaN and YN no doubt hydrolysing in-situ) sintered at 1750 °C under 10 MPa of N_2 for 1 h, gave only a minor amount of C-phase, together with a high proportion of melilite and some wollastonite. These results suggested that C-phase is rich in Si and N with only small amounts of La and Y present. Since the starting powders always contain some oxygen, it is generally difficult to determine whether oxygen is present in the final products.

Ternary nitrides in rare-earth sialon systems have been explored in less detail than in the Y-sialon system, but there are similarities and also differences.[5,6] The crystal structures of $Sm_3Si_6N_{11}$[16] (tetragonal: $a = 9.9931$, $c = 4.8361$ Å) and $LaSi_3N_5$[17] (ortho-rhombic: $a = 7.838$, $b = 11.236$, $c = 4.807$ Å) were reported in the 1980s, the latter being made by reacting together the binary nitrides at 2000 °C under 50 bar N_2. More recently, other $LnSi_3N_5$ (Ln = La–Nd) and $Ln_3Si_6N_{11}$ (Ln = La–Sm) nitrides have been prepared[18] by reacting either lanthanide silicides with nitrogen, or lanthanide metals with $Si(NH)_2$ in nitrogen at 1500–1650 °C. The latter gave single crystals of $Ln_3Si_6N_{11}$ (Ln = Ce,Pr).[19,20]

This paper is concerned with the characterisation of phases of the type referred to as "C" above, occurring in Y–Si–N, Ln–Si–N and related systems and indexing typically on a 6 × 10 Å hexagonal or equivalent pseudo-hexagonal unit cell. Similar X-ray patterns are shown by the group of compounds of the type $MYbSi_4N_7$ (M = Ba,Sr,Eu)[21,22] which are also hexagonal with $a \sim 6.0$, $c \sim 10.0$ Å and, more recently, by the monoclinic structures $M_2Si_4N_6C$ (M = Ho,Tb).[23]

2. Experimental

The present programme of work formed part of a wider exploration of new phases in M_1–M_2–Si–Al–O–N systems where M_1 and M_2 are Group II metals and/or rare earths (including yttrium). In the samples prepared here, the metals used were Ca, Y and La and these were supplied in the form of metal powders (Ca—BDH granules 99.9%, sieved to retain particles <150 μm; La—metal powder (Aldrich—99.9%); Y—supplied as powdered YH_2 (Aldrich B 99.9%), the hydrogen coming off at low temperatures during firing). These were mixed with Si_3N_4 powder (Starck—B7 grade) plus in some runs AlN (Starck Grade B) and Al_2O_3 (Alcoa, Grade A17). The relatively low melting points (Y = 1522, La = 921, Ca = 839 °C) of the metals resulted in the formation of liquid at reaction temperatures which assisted reaction and crystal growth. The La powder was supplied in oil, the latter being removed before use. Powder mixtures were fired in the reducing atmosphere of a carbon resistance furnace at 1700–1900 °C in nitrogen. Some additional experiments using Mg and Al metal powders (BDH–coarse powder and fine flakes, respectively) were also carried out, but in these cases the firing temperature was restricted to ≤1700 °C to prevent volatilisation of gaseous species and the formation of silicides. Further experimental details are given below in the sections relating to the specific compounds prepared.

Samples were analysed by powder XRD using the Hägg-Guinier focusing camera technique; Cu $K\alpha_1$ radiation was used and an internal standard of KCl added. Powder photographs were measured using an automatic line scanner (LS-20) and accompanying SCANPI and PIRUM software. EDX analysis was performed by means of a Hitachi 2400 electron microscope and analyser (Oxford Instruments Microanalysis ISIS-II). Crushed powder samples were carefully examined by transmission optical microscopy to identify good-quality single crystals and diffraction data were collected for these on the Synchrotron Radiation Source at the CLRC Daresbury Laboratory (Station 9.8) using a Bruker SMART 1K CCD. Structure solution and refinement were carried out using the SHELXTL suite of programs and structures were plotted using ATOMS 4.1.

NMR spectra were acquired on a custom-built spectrometer using a magnet with a field strength of $B_0 = 5.9$ T, the relevant resonance frequencies being $\nu_0(^{13}C) = 62.88$ MHz and $\nu_0(^{29}Si) = 49.67$ MHz. A Bruker MAS probe with an outer rotor diameter of 7 mm was used, and the samples were spun at 4.0 kHz (except for the ^{13}C spectra of Y and Ca,Y samples, which were spun at 3.2 kHz). Single-pulse excitation with a tip-angle of $\sim\pi/2$ was used for all spectra and, due to the long T_1 relaxation times of the rigid ceramic samples, a recycle delay of 1 h was applied. For

the ^{13}C spectra, 140 transients were acquired (110 for the La,Y sample) and 92 transients for the ^{29}Si spectra (48 for La,Y and Ca,Y compounds). The spectra were referenced to $(CH_3)_4Si$ via the signals for solid adamantane for ^{13}C, and solid $[(CH_3)_3Si]_4Si$ for ^{29}Si.

3. Results

Table 1 shows the results of firing M:Si_3N_4 mixtures with a starting M:Si ratio of 1:2; numbers in the product columns indicate the relative intensities of the strongest lines. In the case of the yttrium samples there were always inner and outer layers, especially for those fired at the higher temperature of 1900 °C, where the inner layers were the oxygen-containing phases $Y_6Si_{11}N_{20}O$ and $Y_3Si_5N_9O$ and the outer layer was predominantly C-phase. However, in other samples containing La or mixed cations, a random distribution of the main phase(s) was observed, with C-phase and a small amount of $LaSi_3N_5$ and/or $La_3Si_8N_{11}O_4$ (never $La_3Si_6N_{11}$) also present.

3.1. Crystal structure of $La_2Si_4N_6C$

Crystals large enough for structure determination were found on the surface of Sample 3 (Table 1), where a thin yellow coating was mainly C-phase. Powder XRD data (Table 2) indexed very satisfactorily on an orthorhombic unit cell with $a = 6.0360(7)$, $b = 10.1246(9)$, $c = 10.5664(11)$ Å; however, $h\,k\,l$ values obtained from single-crystal data showed a preference for half-integral values along two of the axes (x and z) indicating a high probability of twinning. Initial attempts at structure determination by direct methods using SHELXS, were partially successful, with R1 values dropping below 0.20. The structure at this stage consisted of a distribution of $[N(SiN_3)_4]$ units (four $[SiN_4]$ tetrahedra meeting at a central nitrogen atom) similar to those in the

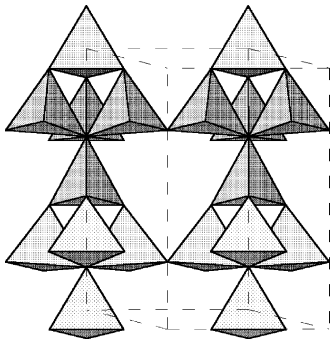

Fig. 1. The $[N(SiN_3)_4]$ present in M(II)M(III)Si_4N_7 nitrides.

(Ba,Sr,Eu)$YbSi_4N_7$ nitrides (Fig. 1) but, whereas in the latter compounds the polar $[N(SiN_3)_4]$ groups all point in the same direction, the present refinement indicated alternate orientations in the $+y$ and $-y$ directions; the same characteristic that has been observed in the $(Ho,Tb)_2Si_4N_6C$ compounds.[23] This difference appeared to be responsible for the lowering of symmetry from hexagonal to orthorhombic. Defining a unique space group at this stage of the refinement proved difficult. From the powder data, the presence of an n glide plane perpendicular to the b-axis appeared convincing, but a b-glide plane associated with z was less so. Three possible space groups were identified ($Pmn2_1$ (31), $P2_1nb$ (33) and $Pmnb$ (62)) but all were equally unsuccessful in reducing the value of R1 below 0.16. At this stage it was noted that large "shadows" of residual electron density existed approximately 0.4 Å from the heavy La atoms, a feature which further substantiated the suspicion that the crystal was twinned. The space group of highest symmetry ($Pmnb$) was selected for further refinement and this terminated at an R1 value of 0.1575 for 844 Fo > 4sig(Fo) and 0.1729 for all 1007 data.

The structure at this stage is illustrated in Fig. 2a, along with that of $BaYbSi_4N_7$ (Fig. 2b); in both figures, just over half the height of the unit cell is illustrated, in order to

Table 1
Experimental results of firing samples with M:(Si,Al) atomic ratios of 1:2

Sample	M	M:Si:Al	T (°C)	Time (h)	C-phase	$Y_6Si_{11}N_{20}O$	$Y_3Si_5N_9O$	$LaSi_3N_5$	Other
(a) Samples prepared from M:Si_3N_4 mixtures									
3 (Main)	La	2:4:0	1700	1	100	–	–	4	–
3 (Crystals)					100	–	–	–	–
4a	La,Y	1.1:4:0	1700	2	100	7	–	2	4
4b			1900	1	100	–	–	–	<2
2	Ca,Y	1.1:4:0	1900	1	100	–	–	–	–
5 (Main)	Y	2:4:0	1900	0.5	100	70	48	–	–
5 (Shell)					100	4	8	–	–
6a	Y	2:4:0	1700	1.5	–	100	4	–	–
6b	Y (+C)	2:4:0	1700	1.5	100	2	12	–	–
(b) Samples with Al also present									
8 (Main)	Y	2:3:1	1700/1450	3/16	–	100	–	–	5
8 (Outer)					100	71	–	–	2
7	La,Y	1.1:3:1	1700	2	100	7	–	–	3
9	La	2:3:1	1700	2.5	31	–	–	–	100

Table 2
X-ray powder diffraction data for $La_2Si_4N_6C$

h k l	d_{calc} (Å)	d_{obs} (Å)	$2\theta_{obs}$ (°)	I_{obs}
0 0 2	5.2832	5.2752	16.793	12
1 0 1	5.2411	5.2442	16.893	13
0 2 0	5.0623	5.0645	17.497	11
0 1 2	4.6838	4.6814	18.941	6
1 1 1	4.6545	4.6562	19.045	17
0 2 1	4.5654	4.5747	19.387	2
1 2 0	3.8787	3.8801	22.901	6
1 1 2	3.7004	3.7033	24.010	3
0 2 2	3.6552	3.6528	24.347	2
1 2 1	3.6412	3.6421	24.420	7
0 1 3	3.3266	3.3261	26.781	3
0 3 1	3.2149	3.2153	27.722	3
1 0 3	3.0421	3.0419	29.337	44
2 0 0	3.0180	3.0180	29.574	22
1 3 0	2.9457	2.9412	30.365	3
1 3 1	2.8375	2.8394	31.481	100
2 1 1	2.7896	2.7899	32.055	1
0 0 4	2.6416	2.6409	33.916	2
2 0 2	2.6206	2.6207	34.186	3
1 2 3	2.6075	2.6070	34.371	47
2 2 0	2.5923	2.5926	34.568	25
1 3 2	2.5728	2.5730	34.840	12
0 1 4	2.5560	2.5552	35.090	15
2 1 2	2.5370	2.5365	35.357	35
0 3 3	2.4368	2.4359	36.869	2
1 1 4	2.3537	2.3540	38.200	6
0 2 4	2.3419	2.3412	38.417	4
2 2 2	2.3272	2.3266	38.668	3
0 4 2	2.2827	2.2822	39.451	5
1 3 3	2.2596	2.2607	39.842	1
2 1 3	2.2352	2.2352	40.316	8
2 3 1	2.2004	2.2001	40.988	6
1 2 4	2.1833	2.1845	41.294	2
1 4 2	2.1351	2.1349	42.299	3
0 3 4	2.0802	2.0803	43.465	6
2 3 2	2.0698	2.0693	43.708	17
2 0 4	1.9877	1.989	45.569	9
3 0 1	1.9765	1.9768	45.867	4
1 3 4	1.9666	1.9655	46.146	4
1 1 5	1.9569	1.9564	46.373	2
2 1 4	1.9505			
0 2 5	1.9502	1.9494	46.549	9
2 4 0	1.9394	1.9393	46.806	5
1 5 1	1.8908	1.8893	48.122	9
2 2 4	1.8502	1.8505	49.197	3
3 2 1	1.8411	1.8409	49.470	3
1 5 2	1.8043	1.8038	50.559	2
0 3 5	1.7911	1.7908	50.952	2
0 0 6	1.7611	1.7615	51.862	5
0 5 3	1.7555	1.7553	52.059	2
3 0 3	1.7470	1.7470	52.325	13
1 3 5	1.7171	1.7179	53.280	2
2 3 4	1.7127	1.7131	53.441	16
3 3 1	1.7055	1.7053	53.705	15
1 0 6	1.6906	1.6932	54.120	1
0 6 0	1.6874	1.6872	54.329	3
0 6 1	1.6663	1.6668	55.049	10
0 2 6	1.6633	1.6615	55.240	9
3 2 3	1.6515	1.6508	55.629	10
3 3 2	1.6425	1.6412	55.983	5
1 6 0	1.6251	1.6246	56.606	3
0 4 5	1.6222	1.6216	56.720	1
0 6 2	1.6074			
0 5 4	1.6071	1.6068	57.291	3
2 5 2	1.6023	1.6027	57.451	15
3 4 0	1.5750	1.5737	58.612	2
1 4 5	1.5666	1.5670	58.887	4
1 6 2	1.5533			
1 5 4	1.5530	1.5528	59.479	4
2 0 6	1.5210	1.5220	60.808	17
4 0 0	1.5090	1.5096	61.362	11
1 6 3	1.4756	1.4758	62.925	3
4 2 0	1.4461	1.4460	64.376	3
3 1 5	1.4423	1.4412	64.616	1
2 4 5	1.4289	1.4294	65.215	4
2 6 2	1.4188	1.4189	65.759	8
2 5 4	1.4185			
3 5 1	1.4144	1.4142	66.005	2
4 2 2	1.3948	1.3947	67.049	1
1 6 4	1.3842	1.3841	67.631	2
2 6 3	1.3588	1.3573	69.153	9
3 4 4	1.3528	1.3522	69.452	1
1 3 7	1.3434	1.3424	70.032	2
2 1 7	1.3382	1.3399	70.182	2
3 3 5	1.3378	1.3356	70.442	5
4 3 2	1.3330	1.3315	70.691	3
3 1 6	1.3139	1.3137	71.796	7
2 4 6	1.3038	1.3026	72.504	5
0 4 7	1.2964	1.2956	72.959	6
1 6 5	1.2883	1.2873	73.506	3
3 6 1	1.2833	1.2834	73.767	3
1 1 8	1.2799	1.2786	74.090	3
1 2 8	1.2503	1.2488	76.168	3
1 8 0	1.2386	1.2377	76.976	4
4 3 4	1.2215	1.2209	78.235	5
3 6 3	1.2137	1.2152	78.673	11

Orthorhombic: $a = 6.0360(7)$, $b = 10.1246(9)$, $c = 10.5664(11)$ Å.

show more clearly the distribution of tetrahedra. As in the (Ba,Sr,Eu)$YbSi_4N_7$ structures, the Si–N bonds not involving the central atom in the $[N(SiN_3)_4]$ units were similar in length and consistent with the sum of the radii of Si and N (~1.7 Å), while bonds involving this central atom were significantly longer (1.88–1.96 Å). In addition, the displacement factor for this atom was much larger than for the other nitrogen atoms. A further observation was that the stoichiometry of $La_2Si_4N_7$ did not demonstrate valency balance, i.e. whereas the unit cell contents of 8 La and 16 Si agreed with the measured EDX La:Si atom ratio of 1:2, the 28 non-metal sites provided too few non-metal valencies for electrical neutrality. By analogy with $(Ho,Tb)_2Si_4N_6C$,[23] it was appreciated that all these observations could be explained if the central atom in the $[N(SiN_3)_4]$ groups was carbon rather than nitrogen, giving a formula of the type $La_2Si_4N_6C$. This has the correct valency balance and accepted values for Si–C bond lengths are consistent with the observed value of 1.9 Å; moreover, carbon is extremely suited to a regular tetrahedral [4]-coordination by silicon. Placing carbon in this site also allowed the displacement factor to refine to a very acceptable value (see Table 3). Refinement of anisotropic temperature factors made little

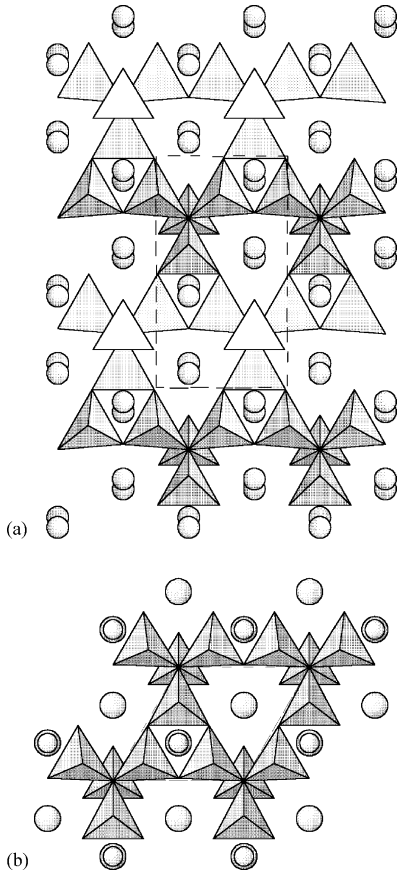

Fig. 2. Crystal structures of (a) $La_2Si_4N_6C$ perpendicular to [0 1 0] and (b) $BaYbSi_4N_7$ perpendicular to [0 0 1] (after Huppertz and Schnick[21]). In the latter, large circles represent Ba, and smaller circles Yb.

difference to the value of R1 (a reduction from 0.1575 to 0.1456), however, whilst the values of U_{11} and U_{33} became 0.0055 and 0.0057, respectively, consistent with isotropic behaviour, U_{22} increased to 0.0838, i.e. in the direction parallel to the *b* axis and consistent with the extended 1.9 Å bond. Final atomic coordinates are listed in Table 3, based on *Pmnb* as the space group; bond lengths and angles are shown in Table 4.

The departure of the structure from the hexagonal symmetry observed for the (Ba,Sr,Eu)$YbSi_4N_7$ phases is due to the alternate inversion of the $[C(SiN_3)_4]$ units, which appears to be a result of the lattice attempting to compensate for the similar sized large cations. In the (Ba,Sr,Eu)$YbSi_4N_7$ structures, the large divalent cations lie in [12]-coordination, with the smaller Yb cations [6]-coordinated; in the present structure, the La atoms are [7]- and [8]-coordinated by nitrogen in the two large cation sites.

Table 4
Bond lengths (Å) and angles (°) for $La_2Si_4N_6C$

La1–N2	2.43(3)	La2–N5	2.55(5)		
La1–N2	2.43(3)	La2–N4	2.62(3)		
La1–N3	2.48(4)	La2–N4	2.62(3)		
La1–N4	2.62(3)	La2–N3	2.74(4)		
La1–N4	2.62(3)	La2–N2	2.94(3)		
La1–N2	2.79(3)	La2–N2	2.94(3)		
La1–N2	2.79(3)	La2–N5	3.02(1)		
		La2–N5	3.02(1)		
Si1–N5	1.60(5)	Si2–N4	1.70(3)	Si3–N3	1.73(3)
Si1–N2	1.76(3)	Si2–N4	1.70(3)	Si3–N4	1.79(3)
Si1–N2	1.76(3)	Si2–N5	1.70(6)	Si3–N2	1.79(3)
Si1–C1	1.92(6)	Si2–C1	1.88(5)	Si3–C1	1.96(4)
N2–Si1–N2	105(2)	N4–Si2–N5	103(2)	N2–Si3–N4	106(2)
N2–Si1–N2	106(2)	N4–Si2–N5	103(2)	N2–Si3–N3	108(2)
N2–Si1–N5	106(2)	N4–Si2–N4	115(2)	N3–Si3–N4	110(2)
N2–Si1–C1	113(2)	N4–Si2–C1	116(2)	N2–Si3–C1	106(2)
N2–Si1–C1	113(2)	N4–Si2–C1	116(2)	N3–Si3–C1	111(2)
N5–Si1–C1	115(3)	N5–Si2–C1	102(3)	N4–Si3–C1	115(2)

The presence of carbon in these samples is not unexpected because they were fired in carbon crucibles and the graphite heating element is also adjacent; moreover, any traces of oil retained from the storage medium for the lanthanum powder would combust to give very reactive carbon. These results also explain why, in the present work, the similar cation ratio compound $La_3Si_6N_{11}$ was never observed; researchers who have prepared this phase have usually done so at lower temperatures in a carbon-free environment. To confirm the presence of carbon in this compound, other techniques were used, and the results of ^{29}Si and ^{13}C NMR analyses obtained for this (and related) compounds are given below.

3.2. Characterisation of $Y_2Si_4N_6C$, $LaYSi_4N_6C$ and $CaYSi_4N_7$

Similar results were obtained when yttrium was used in place of lanthanum in the starting mix as shown in Table 1.

Table 3
Final atomic coordinates for $La_2Si_4N_6C$

Atom	Site/symmetry	*x*	*y*	*z*	Sof	U_{iso} (Å^2)
La1	4*c*/*m*	0.25	0.0911(3)	0.4385(3)	1.0	0.0047(6)
La2	4*c*/*m*	0.25	0.9526(3)	0.3954(3)	1.0	0.0070(7)
Si1	4*c*/*m*	0.25	0.4817(14)	0.7397(11)	1.0	0.0098(22)
Si2	4*c*/*m*	0.25	0.7036(12)	0.9241(10)	1.0	0.0056(21)
Si3	8*d*/*l*	−0.0044(14)	0.7290(9)	0.6700(7)	1.0	0.0050(14)
C1	4*c*/*m*	0.25	0.792(6)	0.768(5)	1.0	0.020(10)
N2	8*d*/*l*	0.020(5)	0.552(3)	0.664(3)	1.0	0.006(3)
N3	4*c*/*m*	0.75	0.769(4)	0.746(3)	1.0	0.006(3)
N4	8*d*/*l*	0.488(4)	0.716(3)	0.009(3)	1.0	0.006(3)
N5	4*c*/*m*	0.25	0.452(6)	0.879(5)	1.0	0.024(10)

Again, the samples showed outer and inner regions, with the outside substantially C-phase and the inside consisting of other phases such as $Y_6Si_{11}N_{20}O$ and $Y_3Si_5N_9O$. A maximum amount of C-phase was observed at the Y:Si ratio of 1:2, consistent with EDX data for the final powder. The X-ray powder pattern[11,12] is very similar to that of $La_2Si_4N_6C$ shown in Table 2, but with systematically decreased d-spacings and unit cell parameters; for sample 6b, $a = 5.9677(7)$, $b = 9.8937(13)$, $c = 10.2648(13)$ Å.

A crystal, mounted for single-crystal structure determination, produced data good enough to confirm a similarity to $La_2Si_4N_6C$ in composition and structure, but refinement was inconclusive due to twinning and imperfections in the crystal. Likewise, use of the monoclinic unit cell reported for the Ho and Tb analogues[23] ($a \sim 5.9$, $b \sim 9.9$, $c \sim 11.9$ Å, $\beta \sim 120°$) made no improvements in the result. For $La_2Si_4N_6C$, it was argued that the carbon could have come from the oil in which the La powder was supplied. This possibility could not have arisen here because the yttrium powder was supplied as YH_2, not immersed in oil, and yet gave the same results. A deliberate addition of carbon powder to the yttrium sample 6b, as compared to a merely stoichiometric mixture (sample 6a), also confirmed clearly the significance of carbon as one of the atomic constituents, since C-phase is very strong in the carbon-containing sample, whilst non-existent in the other (see Table 1). This, combined with the fact that the C-phase is more usually observed on the outside of the sample, strongly suggests that the carbon comes from the CO gas present in the furnace environment.

When half the La is replaced by Y, C-phase is again the main product, with $(Y,La)_6Si_{11}N_{20}O$ and $(La,Y)Si_3N_5$ as minor additional phases. However, in this case C appears at lower temperatures (~1700 °C), which would suggest that the structure forms more readily when mixtures of different-sized cations are used. The powder XRD pattern of this $(La,Y)_2Si_4N_6C$ phase (Table 5) indexes on a hexagonal unit cell of dimensions $a = 6.0072$, $c = 9.8809$ Å, showing it to be isostructural with the $(Ba,Sr,Eu)YbSi_4N_7$ series. Clearly the presence of equal numbers of large and small cations is responsible for the higher symmetry; single crystals of this sample were not available for structure determination.

Table 1 also includes the result of reacting equimolar amounts of Ca and Y powders with silicon powder and nitriding, and again this shows the formation of a C-phase product at 1900 °C. Since the starting composition of $CaYSi_4N_7$ has the same stoichiometry and the large Ca and Y cations have relative atomic radii similar to those in the $(Ba,Sr,Eu)YbSi_4N_7$ series, it was expected that the structures would be identical. However, the low boiling point of calcium caused some loss of Ca by evaporation, and elemental analysis carried out by EDX on the centre of the fired pellet showed the Ca:Y ratio to be not 1:1 but approximately 2:3, resulting in an overall Ca:Y:Si ratio of 0.8:1.2:4.0. With an excess of Y^{3+} relative to Ca^{2+}, valency balance would require additional negative charge. This is easily provided by a small amount of carbon substitution for nitrogen and was explored by ^{13}C NMR analysis (see below). The composition of the sample is therefore $Ca_{0.8}Y_{1.2}Si_4N_{6.8}C_{0.2}$, representing the $x = 0.2$ member of the more general solid solution series $Ca_{(1-x)}Y_{(1+x)}Si_4N_{(7-x)}C_x$. As with the $(La,Y)_2Si_4N_6C$ phase above, the XRD pattern is hexag-

Table 5
X-ray powder diffraction data for $(La,Y)_2Si_4N_6C$

hkl	d_{calc} (Å)	d_{obs} (Å)	$2\theta_{obs}$(°)	I_{obs}
100	5.2024	5.2009	17.034	17
002	4.9405	4.9398	17.942	10
101	4.6033	4.6027	19.268	21
102	3.5824	3.5817	24.838	8
110	3.0036	3.0038	29.717	62
103	2.7828	2.7827	32.140	100
200	2.6012	2.6012	34.450	8
112	2.5665	2.5667	34.928	81
201	2.5155	2.5155	35.662	68
004	2.4702	2.4707	36.331	7
202	2.3018	2.3018	39.102	11
104	2.2314	2.2309	40.397	4
203	2.0413	2.0415	44.334	18
210	1.9663	1.9664	46.123	4
211	1.9285	1.9283	47.089	6
114	1.9079	1.9081	47.618	2
105	1.8474	1.8473	49.288	12
212	1.8269	1.8268	49.878	5
300	1.7341	1.7341	52.744	13
213	1.6883	1.6882	54.294	43
006	1.6468	1.6468	55.776	6
302	1.6363	1.6362	56.169	23
205	1.5736	1.5733	58.628	33
106	1.5700	1.5676	58.862	1
214	1.5384	1.5387	60.080	3
220	1.5018	1.5020	61.706	30
116	1.4440	1.4436	64.496	6
310	1.4429			
222	1.4369	1.4369	64.833	2
311	1.4277	1.4280	65.287	2
304	1.4193	1.4185	65.780	1
215	1.3939	1.3926	67.163	22
206	1.3914			
312	1.3850	1.3850	67.581	1
107	1.3623	1.3625	68.852	1
313	1.3216	1.3212	71.326	21
400	1.3006	1.3001	72.666	1
401	1.2895	1.2892	73.380	6
224	1.2832	1.2837	73.746	20
216	1.2625	1.2617	75.253	5
314	1.2459	1.2451	76.435	1
207	1.2407	1.2404	76.777	2
008	1.2351	1.2348	77.190	1
403	1.2097	1.2096	79.108	1
108	1.2017	1.2015	79.748	3
306	1.1941	1.1936	80.383	2
320	1.1935			
321	1.1849	1.1846	81.120	2
315	1.1653	1.1647	82.807	5
118	1.1423	1.1408	84.941	7
410	1.1352	1.1339	85.581	7
323	1.1221	1.1210	86.808	12

Hexagonal: $a = 6.0072(3)$, $c = 9.8809(6)$ Å.

onal rather than orthorhombic, as expected with different large cations present, and indexed on a unit cell with $a = 5.9874(4)$, $c = 9.7849(8)$ Å. Powder diffraction data and a single-crystal structure determination on this phase are described in the next paper.[24]

X-ray powder diffraction patterns are shown in Fig. 3 for the four main structures studied in this work, namely, (a) $(Ca,Y)_2Si_4N_6(N,C)$ (b) $(La,Y)_2Si_4N_6C$ (c) $Y_2Si_4N_6C$ (d) $La_2Si_4N_6C$. The pattern of $(Ca,Y)_2Si_4N_6(N,C)$ shows an interesting feature compared to the other phases, in that there is no line at ∼18° 2θ. This line represents the (0 0 2) reflection in the basic hexagonal unit cell and can be seen clearly in the other hexagonal structure (b) and also in the orthorhombic structures of (c) and (d). Since the patterns of $BaYbSi_4N_7$ and $SrYbSi_4N_7$ both also contain an (0 0 2) reflection, this absence cannot be attributed merely to the different Si-C or Si–N bonds, but probably arises because of the significantly reduced atomic number of calcium compared with the other large cations used here.

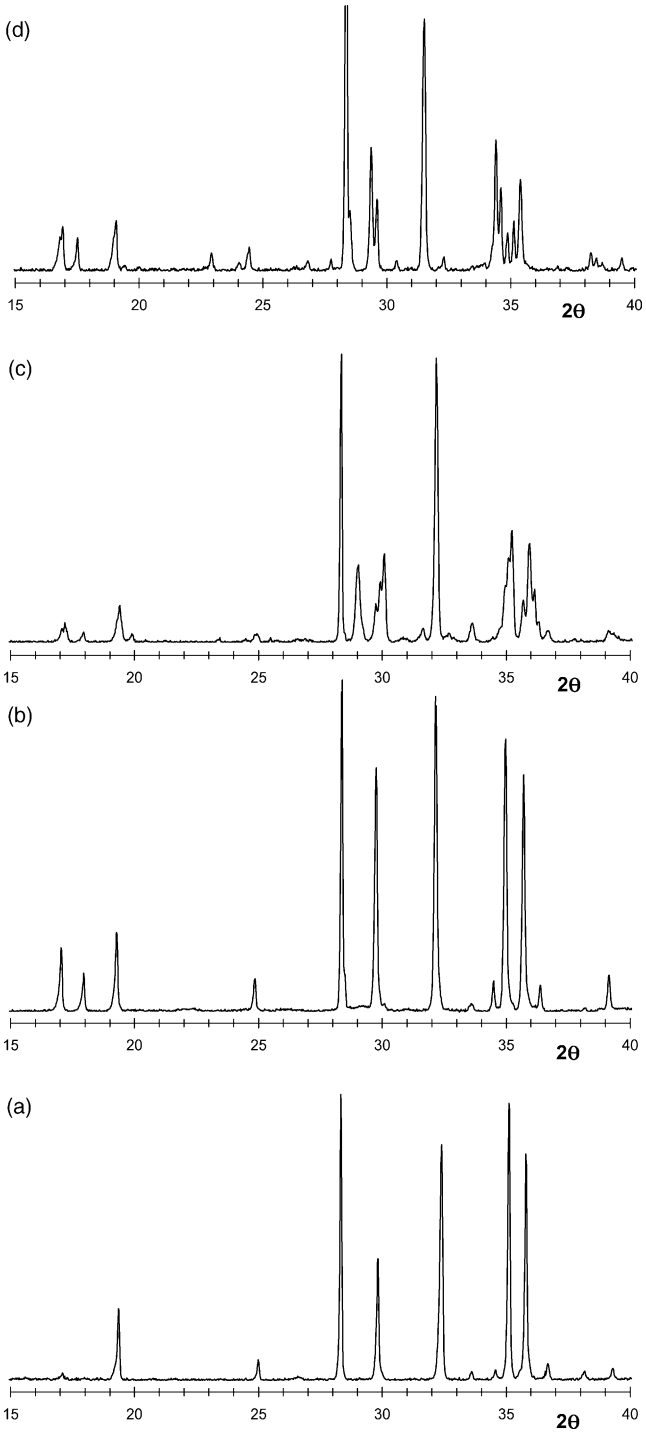

Fig. 3. X-ray powder diffraction patterns for (a) $(Ca,Y)_2Si_4N_6(N,C)$ (b) $(La,Y)_2Si_4N_6C$ (c) $Y_2Si_4N_6C$ (d) $La_2Si_4N_6C$.

3.3. NMR analysis

^{29}Si and ^{13}C MAS spectra for the four carbonitrides characterised in the previous sections are shown in Fig. 4 and the data (including linewidths) summarised in Table 6. For the hexagonal compound $(La,Y)_2Si_4N_6C$, the ^{29}Si spectrum (Fig. 4g) consists of two peaks at $\delta_{Si} = -33.1$ and -39.1 ppm, in the intensity ratio 1:3.6. The silicon atoms in this compound are essentially those in the $[C(SiN_3)_4]$ unit and, even though all of them are surrounded by a $[N_3C]$ environment, three of the sites are related by triad symmetry, whilst the fourth sits uniquely on the triad axis. This would suggest a two-peak ^{29}Si spectrum, in which the peaks are in the intensity ratio of 1:3, which is in quite good agreement with the results observed. The ^{13}C spectrum for this compound (Fig. 4b) shows a single peak at $\delta_C = 36.3$ ppm, consistent with expectations.

The other hexagonal compound, $(Ca,Y)_2Si_4N_6(N,C)$, differs in that the central site of the $[N(SiN_3)_4]$ unit is now occupied by both nitrogen and carbon in the approximate ratio 0.8:0.2. In addition to the 1:3 intensity ratio ^{29}Si spectrum, provided by the 0.2 carbon atoms in this site, the other 0.8 nitrogen atoms also have the same four $[SiN_3]$ units surrounding them; these would give a similar spectrum, but probably shifted to slightly lower frequencies. The overall result would therefore be a four-peak ^{29}Si spectrum, with the intensities of the peaks (normalised to a total of 100%) in the ratio 5(C):20(N):15(C):60(N), where C and N here refer to either C- or N-centred $[(C,N)(SiN_3)_4]$ units respectively. The observed ^{29}Si spectrum (Fig. 4h) is not inconsistent with expectations, if it is assumed that the main peak at $\delta_{Si} = -36.9$ ppm corresponds to the 60N peak above, while the three other peaks are not resolved, but distributed between $\delta_{Si} = -22$ and -36 ppm. The small peak at $\delta_{Si} = -19$ ppm is due to impurity silicon carbide (probably present in such small amount as to be not visible on the XRD spectra), and the unusually sharp feature at $\delta_{Si} = -40$ ppm (which occurs in all the spectra) is an artefact and can be ignored. Prior to carrying out the NMR work, it was expected that the ^{13}C NMR spectrum would not give any peaks because the anticipated composition was $CaYSi_4N_7$, with no carbon present. Fig. 4a shows that this is not the case, and the chemical shift of $\delta_C = 34.0$ ppm is not dissimilar to that of the

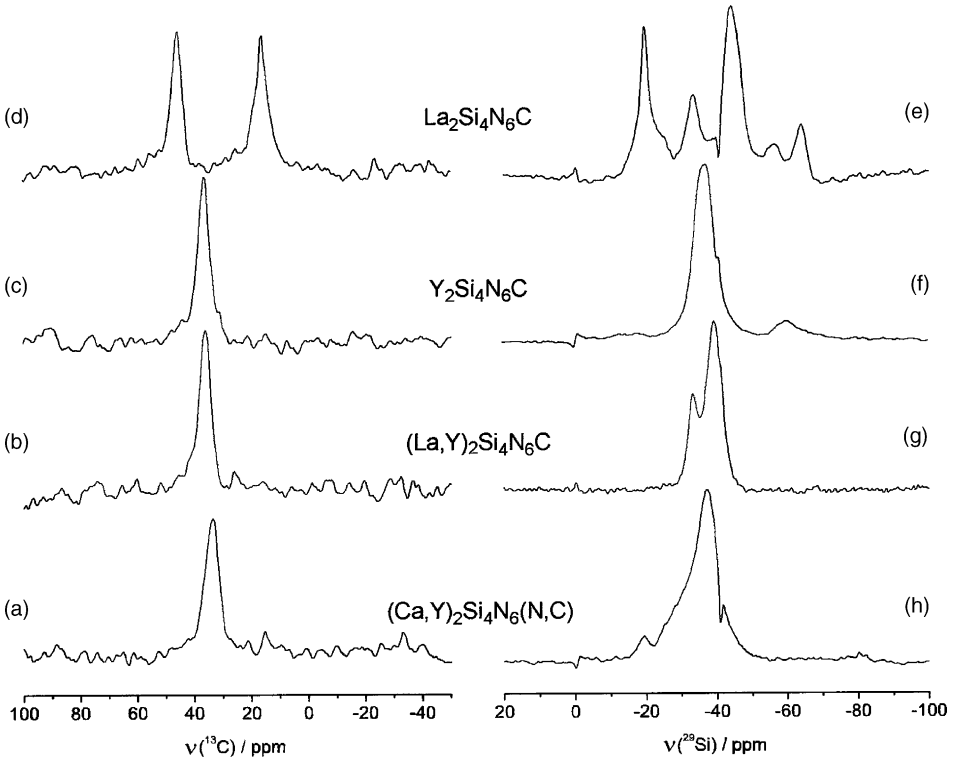

Fig. 4. ^{13}C (a–d) and ^{29}Si (e–h) MAS NMR spectra of the carbonitride samples.

mixed (La,Y) phase ($\delta_C = 36.3$ ppm), showing that carbon is indeed present and is in a similar site in both structures. The intensity of this peak is perhaps higher than expected for the 0.2 carbon atoms per formula unit deduced from the EDX analysis.[24] The small subsidiary peak at 15 ppm corresponds to the small amount of impurity SiC present.

The $La_2Si_4N_6C$ and $Y_2Si_4N_6C$ phases differ from their mixed cation equivalents in having lower symmetry due to the inversion of the [(N,C)(SiN_3)$_4$] units and the adoption of [7]- or [8]-coordination by all the large cations, rather than the [12]/[6] split in the hexagonal modifications. In the ^{29}Si spectrum of $La_2Si_4N_6C$ (Fig. 4e), the two small peaks at $\delta_{Si} = -57$ and -64 ppm are due to $LaSi_3N_5$ impurity present in the sample and the peak at $\delta_{Si} = -20$ ppm arises from silicon carbide impurity (the sample used here for NMR analysis was a different one from that used for the XRD work in Table 1). The remaining two peaks at $\delta_{Si} = -33.2$ and -43.7 ppm are then attributable to the $La_2Si_4N_6C$ phase, and the intensities of these are approximately in the ratio ~1:3.3. In fact the spectrum is not very different from that of the $(La,Y)_2Si_4N_6C$ phase discussed above, but with a slightly larger separation of the two peaks. Despite the symmetry degeneration, the environments of the silicon atoms appear to be not significantly altered, and the spectrum retains a similar appearance. In the ^{13}C spectrum (Fig. 4d), the peak at $\delta_C = 16.1$ ppm is probably due to sil-

Table 6
NMR results for the carbonitride samples

	Transients ($^{13}C/^{29}Si$)	ν_r (kHz) ($^{13}C/^{29}Si$)	δ (ppm) (^{13}C)	lw (Hz)	δ (ppm) (^{29}Si)	lw (Hz)
$La_2Si_4N_6C^{\#}$	144/92	4.0/4.0	16.1, (SiC)	355	−19.7 (SiC)	98
			45.6	305	−43.7	256
					−33.2	170
					−57 (∗)	–
					−63.9 (∗)	125
$Y_2Si_4N_6C$	144/92	3.2/4.0	36.7	300	−37.6	305
					−60 (+)	
$(La,Y)_2Si_4N_6C$	109/48	4.0/4.0	36.3	309	−39.1	228 d
					−33.1	142 d
$(Ca,Y)_2Si_4N_6(N,C)$	140/48	3.2/4.0	34.0	381	−36.9	378
					−19 (SiC)	

d—deconvoluted; lw—linewidth at half-height; (∗) $LaSi_3N_5$; (+) probably $Y_3Si_5N_9O$; (#) a separate sample from that shown in Table 1.

icon carbide, and once again there is a single carbon peak (at $\delta_C = 45.6$ ppm) for the carbonitride phase, in agreement with expectations from the proposed structure, though at a higher chemical shift than for the other carbonitrides.

For the $Y_2Si_4N_6C$ compound, the ^{29}Si spectrum is shown in Fig. 4f. The small feature at $\delta_{Si} = \sim -60$ ppm is due to $Y_3Si_5N_9O$ impurity. This impurity phase was also present in a sample examined by Leach[25] who, at the time, thought it had the composition $Y_2Si_3N_6$; he measured three peaks for the ^{29}Si spectrum in the intensity ratio 2:2:1, occurring at $\delta_{Si} = -57.3$, -60.2 and -64.8 ppm, consistent with our observations. The ^{29}Si spectrum obtained in the present work (Fig. 4f) appears to consist (apart from the impurity peak and the small artefact) of a single resonance at $\delta_{Si} = -37.6$ ppm. However, this is rather broad so presumably the expected two peaks cannot be resolved. Indeed, Leach[25] also examined $Y_2Si_4N_6C$ (at that time thought to be $Y_6Si_3N_{10}$) and found two peaks at $\delta_{Si} = -36.0$ and -38.5 ppm with intensity ratio ~1:1.6, again consistent with our result. The substantial difference in chemical shifts from the spectrum of the $La_2Si_4N_6C$ system is surprising, but may be due to the distortion imposed on the structure by the relatively small size of the yttrium cation compared with that of lanthanum or calcium. Clearly the single peak seen for $Y_2Si_4N_6C$ cannot be due to a uniform [7]- coordination of the cations. The carbon spectrum (Fig. 4c) again gives a single carbon peak at $\delta_C = 36.7$ ppm, in complete agreement with expectations.

4. Discussion

Deviation from 1:1 in the ratio of the large cations in $(Ca,Y)_2Si_4N_6(N,C)$ not only required mixed occupation of one of the large cation sites but also necessitated modifications to the non-metal site occupation scheme to achieve charge neutrality. In fact this is achieved by the introduction of carbon into the central non-metal site of the $[N(SiN_3)_4]$ units as confirmed by ^{13}C NMR spectra. For all the La- and Y-containing samples, it was difficult to prepare single-phase specimens, suitable for single-crystal structure determination. However, in these structures the large cations are all trivalent, so there is no change in electronic charge on altering the cation ratio, and the [4]-coordinated non-metal sites remain fully occupied by carbon. It is therefore probable that a range of orthorhombic solid solutions exists at the ends of the $La_2Si_4N_6C$–$Y_2Si_4N_6C$ pseudo-binary system whilst at a certain composition from both ends of the system, the symmetry changes to hexagonal and this is preserved throughout the central region of the system. A change in the symmetry is readily detectable on X-ray powder diffraction patterns, and therefore the La:Y ratio in such a composition can readily be determined. Fig. 5 shows a plot of the unit cell parameters of the $(M^{II},M^{III})_2Si_4(N,C)_7$ phases prepared in the present work, along with those in the $(Ba,Sr,Eu)YbSi_4N_7$ series, as a function of the mean ionic radius of the large cations in each compound. For the

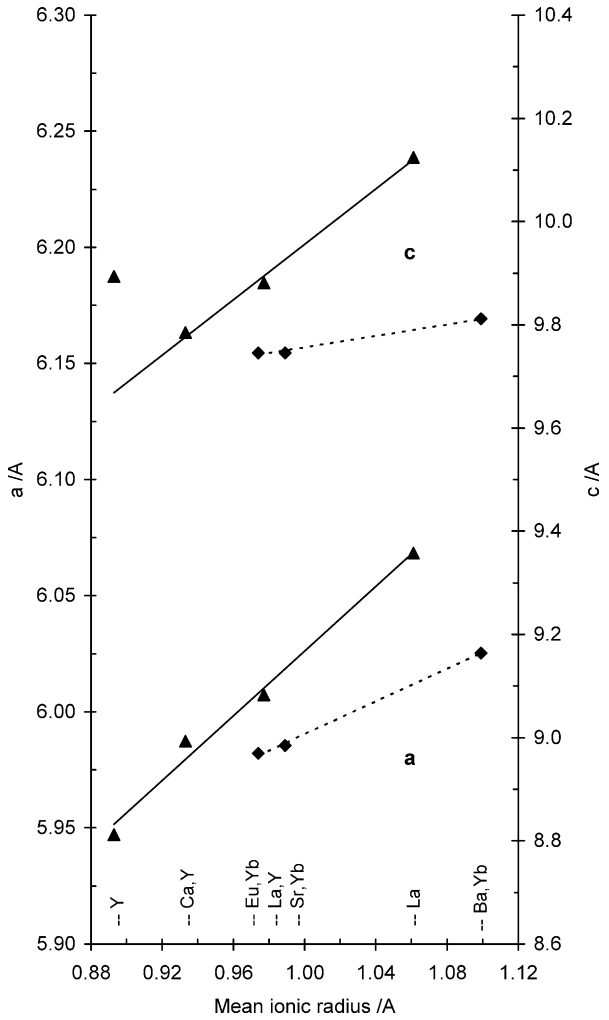

Fig. 5. Unit cell dimensions of $(M^{II},M^{III})_2Si_4(N,C)_7$ phases (M^{II} = Ba,Sr,Eu,Ca; M^{III} = La,Y,Yb) (— present work; --- after Huppertz and Schnick[21,22]).

orthorhombic structures mean values of a and $b/\sqrt{3}$ have been calculated and plotted along with a for the hexagonal structures. All these lie on an approximately straight line, as do the hexagonal parameters of the (Ba,Sr,Eu) samples, demonstrating a linear increase with increasing mean ionic radius. The c parameter of the $Y_2Si_4N_6C$ phase surprisingly, does not fit in with this trend. Attempts to produce a mixed Ca,La or Mg,Y derivative of C-phase were unsuccessful, showing that there is a limit to the range of cation sizes which can be incorporated into this structure. However, if two trivalent cations are used, a pure nitride can result if one Si atom is simultaneously replaced by one Al atom per formula unit. Based on this principle, the three phases of composition $La_2Si_3Al_1N_7$, $Y_2Si_3Al_1N_7$ and $LaYSi_3Al_1N_7$ were prepared (see Table 1). It was noted that in all cases there was an increase in the a parameter and a decrease in the c parameter relative to the non-substituted structures. The former is consistent with the substitution of a maximum of one Al atom for one Si atom, while the latter represents

Table 7
Unit cell dimensions of some $(M^{II},M^{III})_2(Si,Al)_4(N,C)_7$ compounds (M^{II} = Ba,Sr,Eu,Ca; M^{III} = La,Y,Yb)

Sample	*a* (Å)	*b* (Å)	*c* (Å)
$BaYbSi_4N_7$	6.0254(3)		9.8118(7)
$SrYbSi_4N_7$	5.9854(3)		9.7459(9)
$EuYbSi_4N_7$	5.9822(3)		9.7455(4)
$CaYSi_4N_7$[a]	5.9846(4)		9.7861(8)
$LaYSi_4N_6C$[a]	6.0072(3)		9.8809(6)
$LaYSi_3AlN_7$[a]	6.0223(5)		9.8381(11)
$Y_2Si_4N_6C$	5.9677(7)	10.2648(13)	9.8937(13)
$Y_2Si_3AlN_7$[a]	5.9863(7)	10.2797(15)	9.8449(14)
$La_2Si_4N_6C$	6.0307(7)	10.5664(11)	10.1246(9)
$La_2Si_3AlN_7$[a]	6.0538(8)	10.5773(24)	10.1209(12)

[a] Idealised compositions (see text).

an equivalent substitution of N for C. Measured unit cell parameters are shown in Table 7; the accompanying compositions are idealised for the purpose of illustration only.

5. Conclusions

Experiments have confirmed that series of compounds of the type $M^{III}M^{III}Si_4N_6C$ and $M^{II}M^{III}(Si,Al)_4(N,C)_7$ can be formed by the nitriding of La, Y, and/or Ca metal mixtures in the presence of Si (and Al). Where a large divalent cation is present along with a smaller trivalent cation the structure is hexagonal and consists of regularly spaced $[N(SiN_3)_4]$ tetrahedral groups linked together, with the large cations inserted in the interstices. In compositions where both cations are trivalent, such as La and/or Y, valency balance is preserved by the substitution of C for N in the central [4]-fold site of the resulting $[C(SiN_3)_4]$ group, as confirmed by carbon-13 magic-angle spinning NMR. In addition, where both cations are of similar atomic radius, the structure changes to give a lower orthorhombic symmetry. As an alternative to carbon substitution, the extra valency can be compensated for by replacing one Si atom by Al to allow the formation of pure nitrides of the type $(Y,Ln)_2Si_3AlN_7$. Clearly, numerous other compositional permutations are possible in this group of structures.

Acknowledgements

The authors wish to thank Mr. Marco Ferrazzi for preparation of some La-containing samples and Dr. Simon J. Teat for assistance and crystallographic advice at the CLRC Daresbury Laboratory; also EPSRC for funding during the course of this work under research grant GR/L79625.

References

1. Felsche, J., The crystal chemistry of the rare earth silicates. *Struct. Bond.* 1973, **13**, 100–196.
2. Rae, A. W. J. M., Thompson, D. P., Jack, K. H., The role of additives in the densification of nitrogen ceramics. In *Proceedings of the Fifth Army Materials Technology Conference on "Ceramics for High Performance Applications-II"*, Newport, RI, ed. J. J. Burke, E. N. Lenoe and R. N. Katz. Brook Hill Pub. Co., Chestnut Hill, MA, 1977, pp. 1039–1067.
3. Wills, R. R., Stewart, R. W., Cunningham, J. A. and Wimmer, J. M., The silicon lanthanide oxynitrides. *J. Mater. Sci.* 1976, **11**, 749–759.
4. Marchand, R., Jayaweera, A., Verdier, P. and Lang, J., Preparation and characterisation of new oxynitrides in the Ln–Si–O–N system, melilites $Ln_2Si_3O_3N_4$ and cuspidines $Ln_4Si_2O_7N_2$. *C. R. Hebd. Seances Acad. Sci. Ser. C.* 1976, **283**(15), 675–677.
5. Slasor, S., Liddell, K. and Thompson, D. P., The role of Nd_2O_3 as an additive in the formation of α′ and β′ sialons. In "*Special Ceramics 8*", *British Ceramic Proceedings 37*, ed. S. P. Howlett and D. Taylor. Institute of Ceramics, Stoke-on-Trent, UK, 1986, pp. 51–64.
6. Buang, K. B., *The Magnesium, Cerium and Zirconium Sialons*. Ph.D. thesis, University of Newcastle, 1979, p. 52.
7. Mitomo, M., Izumi, F., Horiuchi, S. and Matsui, Y., Phase relationships in the system Si_3N_4–SiO_2–La_2O_3. *J. Mater. Sci.* 1982, **17**, 2359–2364 (JCPDS 36-570).
8. Thompson, D. P., Leach, M. J. and Harris, R. K., NMR studies of nitrogen ceramics. In *Advanced Structural Materials, Proceedings of the C-MRS International '90*, ed. Y. Han. Elsevier Science, Oxford, UK, 1991, pp. 435–440 (JCPDS 48-1597).
9. Thompson, D. P., Phase relationships in Y–Si–Al–O–N ceramics. In *Materials Science Research, Tailoring Multiphase and Composite Ceramics, Vol 20*, ed. R. E. Tressler, G. L. Messing, C. G. Pantono and R. E. Newnham. Plenum Press, New York, 1985, pp. 79–92.
10. Woike, M. and Jeitschko, W., Preparation and crystal structures of the rare earth nitrido-oxosilicates and nitridosilicates with the general formula $R_{6+x/3}Si_{11}N_{20+x}O_{1-x}$ and the ideal compositions $R_6Si_{11}N_{20}O$ and $R_{6.33}Si_{11}N_{21}$, respectively (R = Y and Gd-Lu). *J. Sol. St. Chem.* 1997, **129**, 312–319 (see also JCPDS 49-1798, $Ho_6Si_{11}N_{20}O$).
11. Liddell, K. and Thompson, D. P., The crystal structure of $Y_3Si_5N_9O$ and revision of the compositions of some high nitrogen-containing M–Si–O−N (M = Y, La) phases. *J. Mater. Chem.* 2001, **11**, 507–512.
12. Ekström, T.C., MacKenzie, K. J. D., Ryan, M. J., Brown, I. W. M. and White, G. V., Phases occurring in the Si_3N_4–YN system. *J. Mater. Chem.* 1997, **7**(3), 505–509.
13. Cao, G. Z., Huang, Z. K. and Yan, D. S., Phase relationships in the Si_3N_4–Y_2O_3–La_2O_3 system. *Sci. China (Ser. A)* 1989, **32**(4), 429–433.
14. Huang, Z. K., Cao, G. Z., Wang, P. L. and Yan, D. S., Phase relationships in the systems Si_3N_4–Y_2O_3–R_2O_3 (R = La,Gd,Yb) and formation of new silicon oxynitrides of rare earth elements. *Unpublished Work, Presented at "Shanghai Symposium and Exhibition of New Ceramics"*, Shanghai, China, April 16–18, 1991.
15. Perera, D. S., Liddell, K., Moricca, S., Drennan, J., Ding, W. and Fan, Q. S., Phase relationships in the Si_3N_4–SiC–La_2O_3–Y_2O_3–SiO_2 system under high pressure gas processing. In *Mass and Charge Transport in Ceramics, Ceramic Transactions, Vol 71*, ed. K. Koumoto, L. M. Shepherd and H. Matsubara. 1996, pp. 539–552.
16. Gaudé, J., Lang, J. and Louer, D., $Sm_3Si_6N_{11}$, Un nouveau nitrure double de silicium et de terre rare. *Rev. Chim. Min.* 1983, **20**, 523–527.
17. Inoue, Z., Mitomo, M. and Ii, N., A crystallographic study of a new compound of lanthanum silicon nitride, $LaSi_3N_5$. *J. Mater. Sci.* 1980, **15**, 2915–2920.
18. Woike, M. and Jeitschko, W., Preparation and crystal structure of the nitridosilicates $Ln_3Si_6N_{11}$ (Ln = La, Ce, Pr, Nd, Sm) and $LnSi_3N_5$ (Ln = Ce, Pr, Nd). *Inorg. Chem.* 1995, **34**, 5105–5108.
19. Schlieper, T. and Schnick, W., Nitrido-silicates III (1)—high-temperature synthesis crystal structure and magnetic properties of $Ce_3[Si_6N_{11}]$. *Zeit. Anorg. Allg. Chem.* 1995, **621**, 1535–1538.

20. Schlieper, T. and Schnick, W., Crystal structure of tripraesiodymium hexasiliconundecanitride, $Pr_3Si_6N_{11}$. *Zeit. Krist.* 1996, **211**(4), 254.
21. Huppertz, H. and Schnick, W., Synthesis crystal structure and properties if the nitridosilicates $SrYbSi_4N_7$ and $BaYbSi_4N_7$. *Z. Anorg. Allg. Chem.* 1997, **623**, 212–217.
22. Huppertz, H. and Schnick, W., $Eu_2Si_5N_8$ and $EuYbSi_4N_7$: the first nitrido-silicates with a divalent rare earth metal. *Acta Crystallogr.* 1997, **C53**, 1751–1753.
23. Höppe, H.A., Kotzyba, G., Pöttgen, R. and Schnick, W., High-temperature synthesis, crystal structure, optical properties, and magnetism of the carbidonitridosilicates $Ho_2[Si_4N_6C]$ and $Tb_2[Si_4N_6C]$. *J. Mater. Chem.* 2001, **11**, 3300–3306.
24. Liddell, K., Thompson, D. P. and Teat, S. J., $M_2(Si,Al)_4(N,C)_7$ (M = La,Y,Ca) carbonitrides—II. The crystal structure of $Ca_{0.8}Y_{1.2}Si_4N_{6.8}C_{0.2}$. *J. Eur. Ceram. Soc.* 2005, **25**, 49–54.
25. Leach, M. J., *Synthesis and Multinuclear Magnetic Resonance Studies of Some Nitrogen-Containing Ceramic Phases*. Ph.D. thesis, 1990, University of Durham.